Propene Polymerization with the Isospecific, Highly Regioselective *rac*-$Me_2C(3$-*t*-Bu-1-Ind$)_2ZrCl_2$/MAO Catalyst. 2. Combined DFT/MM Analysis of Chain Propagation and Chain Release Reactions

Gilberto Moscardi* and Luigi Resconi

Centro Ricerche G. Natta, Basell Polyolefins, P. le G. Donegani 12, I-44100 Ferrara, Italy

Luigi Cavallo

Dipartimento di Chimica, Università di Napoli, Via Cintia, I-80126 Napoli, Italy

Received August 7, 2000

Downloaded by CARLI CONSORTIUM on June 29, 2009
Published on April 11, 2001 on http://pubs.acs.org | doi: 10.1021/om000680e

A combined DFT/MM analysis has been carried out on the chain propagation steps and on possible mechanisms for the formation of unsaturations in propene polymerization catalyzed by *rac*-$Me_2C(3$-*t*-Bu-1-Ind$)_2ZrCl_2$/methylalumoxane (**1**/MAO). The results are compared to the available experimental data on its polymerization performance. The insertion of the *si* propene enantioface at the *R,R* site is favored by 4.0−6.0 kcal/mol, in good agreement with the (slightly underestimated) experimental value of 4.6 kcal/mol. Mechanistic aspects related to highly hindered catalysts are also discussed. The large amount of allyl end groups measured in *i*-PP produced at any [propene] can be rationalized, especially at the highest monomer concentration, by allylic activation of a coordinated propene; allyl end groups formed by this route add to those formed by the unimolecular β-Me transfer reaction. Chain release mechanisms involving a coordinated propene (allylic activation and β-H transfer) kinetically compete. The relatively high rate of chain-end epimerization observed for this catalyst, as well as the presence of internal vinylidene groups, can be rationalized by the relatively high stability of the product of β-H transfer to the metal due to a $H_2C-H\cdots Zr$ agostic interaction. Allylic activation of the growing chain end followed by propene insertion is the source of internal vinylidene unsaturations, but likely not of epimerization. Calculations support the hypothesis that the allylic chain end activation could also occur upon β-H transfer to a coordinated monomer; hence, the formation of internal vinylidenes could also proceed without developing H_2. Finally, we conclude that within the single-center, two-state catalyst model developed to account for the nonlinear activity/[M] relationship, the fast propagating site is the $Zr-CH_2CH(CH_3)P$, while the $Zr-C(CH_3)_2P$ (tertiary alkyl) formed during the course of chain epimerization, proposed by Busico, represents a suitable model for the catalyst resting state.

Introduction

Two of the best studied isospecific *ansa*-zirconocene catalysts for propene polymerization are *rac*-$Me_2C(3$-*t*-Bu-1-Ind$)_2ZrCl_2$/methylalumoxane and *rac*-$C_2H_4(1$-Ind$)_2$-$ZrCl_2$/methylalumoxane (**1**/MAO and **2**/MAO in Chart 1).[1−3] **1**/MAO is particularly interesting since it is both fairly isospecific and perfectly regioselective. With the aim of explaining the available set of experimental data in terms of mechanisms of chain propagation and release, we have carried out a combined DFT/molecular mechanics investigation on **1**.

Before describing our theoretical results, we briefly review the most important features already reported for the system **1**/MAO.

Chart 1

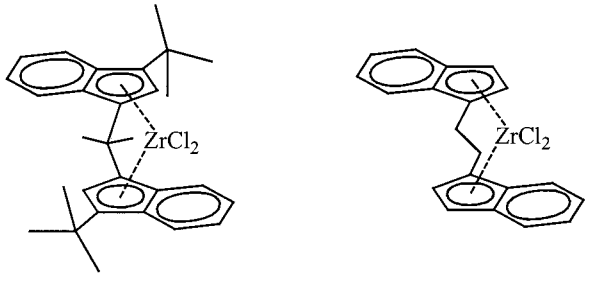

1 (*R,R*)-$Me_2C(3$-*t*-Bu-1-Ind$)_2ZrCl_2$

2 (*R,R*)-$C_2H_4(1$-Ind$)_2ZrCl_2$

Propagation and Isotacticity. The activity of **1**/MAO increases in a nonlinear fashion with increasing propene concentration.[3,4] We have recently discussed how the

(1) Resconi, L.; Cavallo, L.; Fait, A.; Piemontesi, F. *Chem. Rev.* **2000**, *100*, 1253.

(2) Resconi, L.; Piemontesi, F.; Camurati, I.; Sudmeijer, O.; Nifant'ev, I. E.; Ivchenko, P. V.; Kuz'mina, L. G. *J. Am. Chem. Soc.* **1998**, *120*, 2308.

(3) Camurati, I.; Fait, A.; Piemontesi, F.; Resconi, L.; Tartarini, S. *ACS Symp. Ser.* **2000**, *No. 760*, 174.

(4) Resconi, L.; Fait, A.; Piemontesi, F.; Camurati, I.; Moscardi, G. Manuscript in preparation.

10.1021/om000680e CCC: $20.00 © 2001 American Chemical Society
Publication on Web 04/11/2001

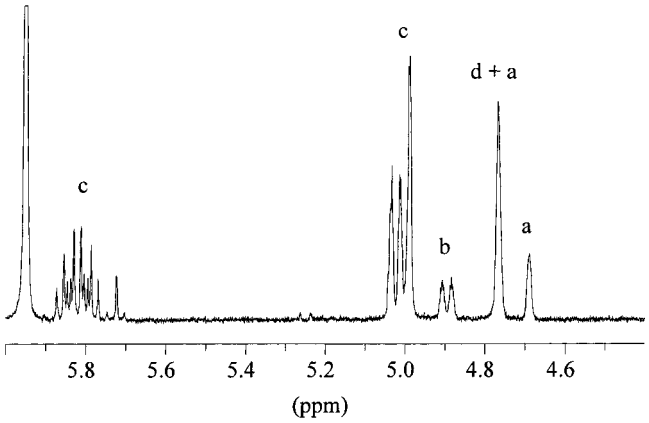

Figure 1. Olefin region of the ^{1}H NMR spectrum ($C_2D_2Cl_4$, 120 °C) of *i*-PP prepared with 1/MAO at 70 °C in liquid propene. Reference: C_2HDCl_4 at 5.95 ppm.

nonlinear activity/[M] relationship can be explained by a single-center, two-state catalyst model, where the active metal centers can exist in two states having different propagation rate constants and which can interconvert without monomer assistance.[5]

1/MAO is both fairly isospecific and highly regioselective (no secondary propene units being detectable by ^{13}C NMR), producing *i*-PP with $\Delta\Delta E^{\ddagger}_{enant} = 4.6$ kcal/mol and a remarkably high $\Delta\Delta E^{\ddagger}_{release}$ of 10.7 kcal/mol.[2,3,6] As is common for metallocene catalysts, its isospecificity is adversely affected by decreasing [propene]: the [*mmmm*] of *i*-PP decreases on going from liquid monomer to [propene] → 0, due to unimolecular primary-growing-chain-end epimerization. The extent of epimerization at a given [M] depends on the polymerization temperature and on the nature of the *ansa* π-ligand.[7−12] For example, **1**/MAO is more stereoselective than **2**/MAO, at any [propene]. Moreover, we have estimated for **1**/MAO that as much as 10% of the stereoerrors observed in liquid propene polymerization at 50 °C are due to epimerization.[3] Hence, since the rate of epimerization increases with temperature,[9,11,12] the above value of 4.6 kcal/mol for $\Delta\Delta E^{\ddagger}_{enant}$ must be overestimated. In the following we will show that the catalyst activity vs monomer concentration and the catalyst stereoselectivity vs monomer concentration profiles could be connected by the same mechanisms.

Analysis of Unsaturations. The proton spectra of *i*-PP samples from **1**/MAO show the presence of four different olefinic groups. The olefinic region of the proton spectrum of a representative sample (T_p = 70 °C, [M] = 9 mol/L) is shown in Figure 1. The corresponding olefin structures, assigned as previously described,[2,3,6,13−15] are shown in Chart 2.

Chart 2. Unsaturated End Group and Internal Vinylidene Structures Identified in *i*-PP Samples from 1/MAO

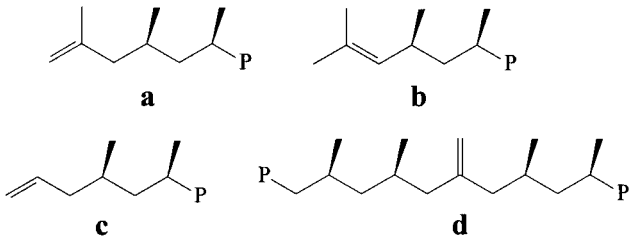

The allyl end group (**c**) always prevails over any other end groups, at any [propene]. The vinylidene end group (**a**) gives a minor contribution to the chain ends, and its fraction decreases by lowering [propene]. The large contribution from the internal vinylidene,[14] structure **d**, and the presence of isobutenyl end groups (**b**)[2,3,6] are noteworthy. Internal vinylidenes increase by increasing [propene]. The fraction of isobutenyl end groups remains approximately constant with [propene], about 20% of the end groups.

The mechanisms for the formation of unsaturations in propene polymerization, several well established, and those proposed on the basis of known organometallic reactions, are reviewed in the following.

(A) Vinylidene (a). This most common end group can be formed by three different mechanisms (Scheme 1).

Mechanism a_1, unimolecular: β-H transfer to the metal, followed by dissociation or associative displacement by a new monomer molecule (a_1').

Mechanism a_2, bimolecular: β-H transfer to a coordinated monomer.

(B) Isobutenyl (b). This is shown in Scheme 2.

Mechanism b_1, unimolecular: formation of a tertiary alkyl species, followed by β-H transfer from the CH_2.[2]

Mechanism b_2: allylic activation of the chain with H_2 release and proton transfer to the CH_2 of the allylic species.

(C) Allyl (c). The presence of the allyl end group suggests that β-CH_3 transfer, at least at low [propene],[16−26] is an important chain release reaction in propene polymerization with **1**/MAO.[13,27] This end

Downloaded by CARLI CONSORTIUM on June 29, 2009
Published on April 11, 2001 on http://pubs.acs.org | doi: 10.1021/om000680e

(5) Fait, A.; Resconi, L.; Guerra, G.; Corradini, P. *Macromolecules* **1999**, *32*, 2104.
(6) Resconi, L.; Piemontesi, F.; Nifant'ev, I. E.; Ivchenko, P. V. PCT Int. Appl. Pat. WO 96/22995 (to Montell), 1996.
(7) Busico, V.; Cipullo, R. *J. Am. Chem. Soc.* **1994**, *116*, 9329.
(8) Busico, V.; Cipullo, R.; Chadwick, J. C.; Modder, J. F.; Sudmeijer, O. *Macromolecules* **1994**, *27*, 7538.
(9) Busico, V.; Cipullo, R. *J. Organomet. Chem.* **1995**, *497*, 113.
(10) Busico, V.; Caporaso, L.; Cipullo, R.; Landriani, L.; Angelini, G.; Margonelli, A.; Segre, A. L. *J. Am. Chem. Soc.* **1996**, *118*, 2105.
(11) Busico, V.; Brita, D.; Caporaso, L.; Cipullo, R.; Vacatello, M. *Macromolecules* **1997**, *30*, 3971.
(12) Busico, V.; Cipullo, R.; Caporaso, L.; Angelini, G.; Segre, A. L. *J. Mol. Catal.* **1998**, *128*, 53.
(13) Resconi, L. *Polym. Mater. Sci. Eng.* **1999**, *80*, 421.
(14) Resconi, L.; Camurati, I.; Sudmeijer, O. *Top. Catal.* **1999**, *7*, 145.
(15) Resconi, L.; Piemontesi, F.; Sudmeijer, O. *Polym. Prepr. Am. Chem. Soc., Div. Polym. Chem.* **1997**, *38*(1), 776.
(16) We did not unambiguously prove that allyl end groups in *i*-PP from **1**/MAO originate from β-CH_3 transfer. However, the occurrence of unimolecular β-CH_3 transfer has been unambiguously established for a large number of similar systems.[17−26] A second possible source of allyl end groups is the allylic activation of a coordinated propene monomer.[28−31] This bimolecular mechanism is discussed further on in the text.
(17) Watson, P. L.; Roe, D. C. *J. Am. Chem. Soc.* **1982**, *104*, 6471.
(18) Eshuis, J. J. W.; Tan, Y. Y.; Teuben, J. H.; Renkema, J. *J. Mol. Catal.* **1990**, *62*, 277.
(19) Eshuis, J. J. W.; Tan, Y. Y.; Meetsma, A.; Teuben, J. H.; Renkema, J.; Evens, G. G. *Organometallics* **1992**, *11*, 362.
(20) Resconi, L.; Piemontesi, F.; Franciscono, G.; Abis, L.; Fiorani, T. *J. Am. Chem. Soc.* **1992**, *114*, 1025.
(21) Yang, X.; Stern, C. L.; Marks, T. J. *Angew. Chem., Int. Ed. Engl.* **1992**, *31*, 1375.
(22) Kesti, M.; Waymouth, R. M. *J. Am. Chem. Soc.* **1992**, *114*, 3565.
(23) Mise, T.; Kageyama, A.; Miya, S.; Yamazaki, H. *Chem. Lett.* **1991**, 1525.
(24) Yang, X.; Stern, C. L.; Marks, T. J. *J. Am. Chem. Soc.* **1994**, *116*, 10015.
(25) Hajela, S.; Bercaw, J. E. *Organometallics* **1994**, *13*, 1147.
(26) Guo, Z.; Swenson, D.; Jordan, R. *Organometallics* **1994**, *13*, 1424.

Scheme 1

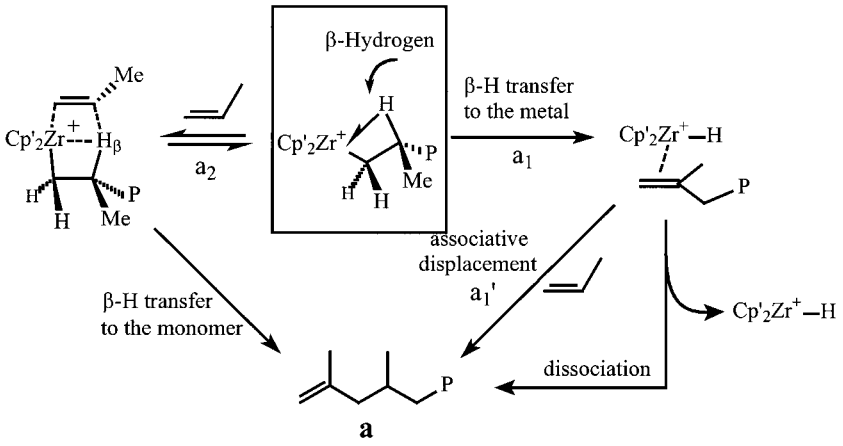

Scheme 2

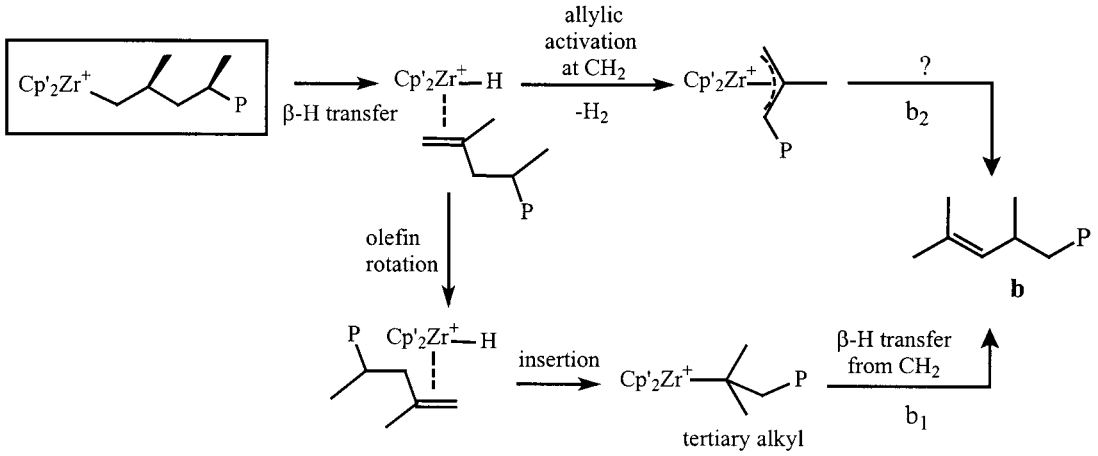

Downloaded by CARLI CONSORTIUM on June 29, 2009
Published on April 11, 2001 on http://pubs.acs.org | doi: 10.1021/om000680e

group can be formed by following the different mechanisms shown in Scheme 3.

Mechanism c_1, unimolecular: β-CH_3 transfer to the metal, followed by dissociation or associative displacement by a new monomer molecule (c_1').

Mechanism c_2, bimolecular: β-CH_3 transfer to a coordinated monomer.

Mechanism c_3, bimolecular: allylic activation of a coordinated propene, followed by chain propagation into the Zr(allyl) species, as observed by Marks and Richardson.[28−31]

(D) Internal vinylidene (d). This is shown in Scheme 4.

Mechanism d_1, unimolecular: allylic activation of the polymer chain, followed by H_2 release and chain propagation into the Zr(2-P-allyl) site.

Mechanism d_2, bimolecular: β-H transfer to a coordinated monomer, followed by allylic activation of the terminated polymer chain and release of a propane molecule.

The mechanism d_3 (insertion of an allyl-terminated polymer chain into the Zr−polymer site, followed by β-H transfer to the metal, Scheme 4), or the σ-bond metathesis reaction suggested by us earlier,[2] which would lead to an internal vinylidene near to the chain end, have been ruled out by ^{1}H NMR analysis and are not further discussed here.

Models and Methods

In this paper, as in part 1 of this work,[32] we limit our studies to models for "naked" cations, that is without accounting for the effects of the counterion as well as that of the solvent.

Recent DFT calculations by Ziegler and co-workers[33] showed that the interactions between the cationic metallocene and the counterion is strongly dependent on the polarity of the solvent and that for solvent with a relatively high dielectric costant (ϵ ca. 10) the counterion could be not bonded to the metallocene. Moreover, all the simulations reported so far on the metallocene/counterion interactions[34−38] were performed on models including the Cp ligands, while in the present paper we

(27) Resconi, L. *J. Mol. Catal.* **1999**, *146*, 167.
(28) Jeske, G.; Lauke, H.; Mauermann, H.; Swepston, P. N.; Schumann, H.; Marks, T. J. *J. Am. Chem. Soc.* **1985**, *107*, 8091.
(29) Christ, C. S.; Eyler, J. R.; Richardson, D. E. *J. Am. Chem. Soc.* **1990**, *112*, 596.
(30) Guyot, A.; Spitz, R.; Journaud, C. *Polym. Prepr. Am. Chem. Soc., Div. Polym. Chem.* **1994**, *35*, 671.
(31) Guyot, A.; Spitz, R.; Journaud, C. In *Catalyst Design for Tailor-Made Polyolefins*; Stud. Surf. Sci. Catal. 89; Soga, K., Terano, M., Eds.; Elsevier: Amsterdam, 1994; p 43.
(32) Moscardi, G.; Piemontesi, F.; Resconi, L. *Organometallics* **1999**, *18*, 5264.
(33) Chan, M. S. W.; Ziegler, T. *Organometallics* **2000**, *19*, 5182.
(34) Fusco, R.; Longo, L.; Masi, F.; Garbassi, F. *Macromolecules* **1997**, *30*, 7673.
(35) Fusco, R.; Longo, L.; Proto, A.; Masi, F.; Garbassi, F. *Macromol. Rapid Commun.* **1997**, *18*, 433.
(36) Fusco, R.; Longo, L.; Proto, A.; Masi, F.; Garbassi, F. *Macromol. Rapid Commun.* **1998**, *19*, 257.
(37) Lanza, G.; Fragalà, I. L.; Marks, T. J. *J. Am. Chem. Soc.* **1998**, *120*, 8257.

Downloaded by CARLI CONSORTIUM on June 29, 2009
Published on April 11, 2001 on http://pubs.acs.org | doi: 10.1021/om000680e

Scheme 3

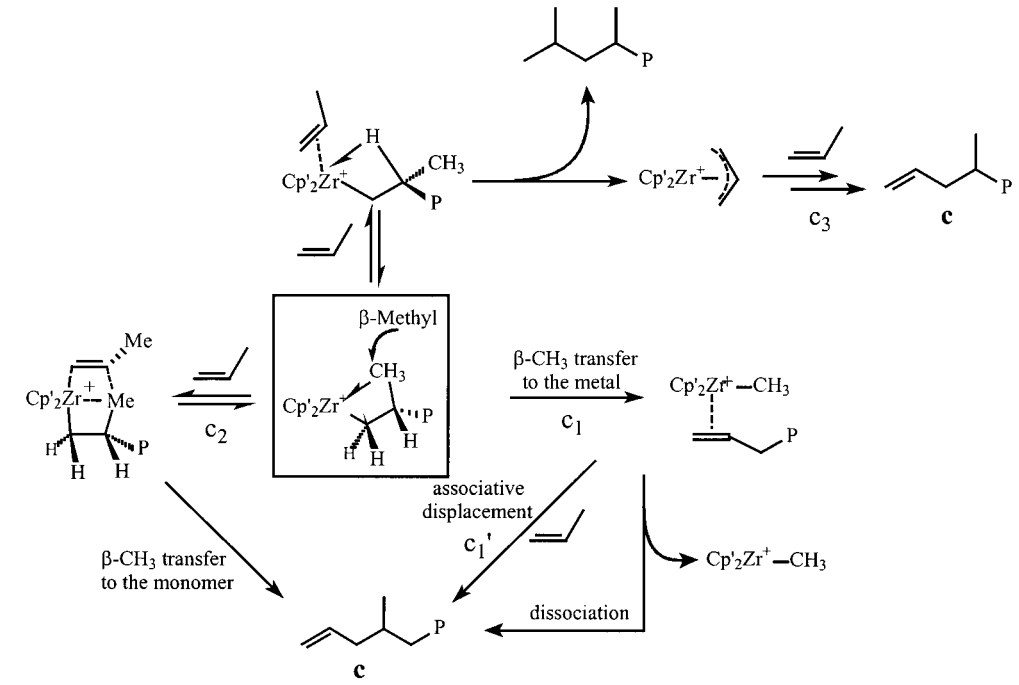

Scheme 4

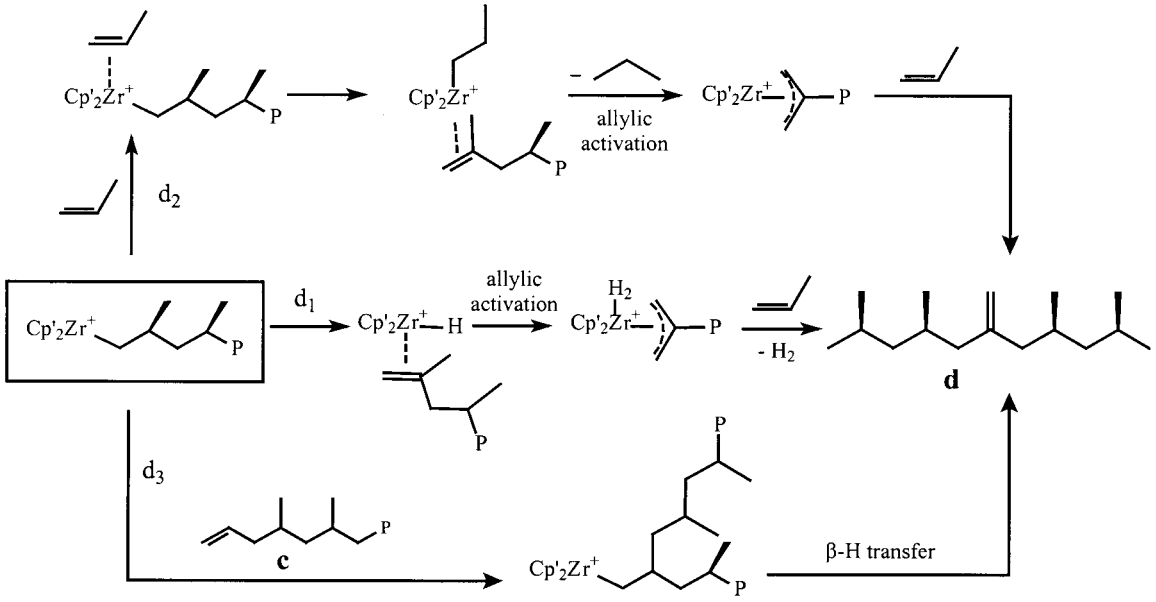

considered the much bulkier metallocene **1**. It is reasonable to assume that the six-membered rings of the indenyls, the bulky *tert*-butyl groups, and the growing chain are able to shield the metal atom from coordination of the counterion. In this respect, we only anticipate that even coordination of the small propene molecule is quite difficult on this metallocene.

The elements of chirality which are relevant for the present study are briefly recalled, to indicate the used terminology. First of all, upon coordination the prochiral propene molecule gives rise to nonsuperimposable *si* and *re* coordinations.[39] A second element of chirality is the configuration of the tertiary carbon atom of the growing chain nearest to the metal atom, which will be described according to the Cahn, Ingold, and Prelog *R*,*S* nomenclature. The saturated growing polymer chain is modeled with the 2-methylbutyl group of both *R* and *S* chiralities, which stem from the insertion of a *si*- or *re*-coordinated propene, respectively. For the sake of simplicity, we refer to the 2-methylbutyl group of *R* and *S* chirality as *si* and *re* chains, respectively. A third element of chirality is that of the catalytic site, which arises from the chirality of coordination of the aromatic $Me_2C(3\text{-}t\text{-Bu-1-Ind})_2$ ligand. In this case, we use the notation *R* or *S*, in parentheses, according to the Cahn–Ingold–Prelog rules[40,41] extended by Schlögl.[42] Without

(38) Chan, M. S. W.; Vanka, K.; Pye, C. C.; Ziegler, T. *Organometallics* **1999**, *18*, 4624.

(39) Hanson, K. R. *J. Am. Chem. Soc.* **1966**, *88*, 2731.

(40) Cahn, R. S.; Ingold, C.; Prelog, V. *Angew. Chem., Int. Ed. Engl.* **1966**, *5*, 385.

(41) Prelog, V.; Helmche, G. *Angew. Chem., Int. Ed. Engl.* **1982**, *21*, 567.

loss of generality, all the calculations here reported refer to models with the *R,R* chirality of coordination of the $Me_2C(3\text{-}t\text{-}Bu\text{-}1\text{-}Ind)_2$ ligand.

Stationary points on the potential energy surface were calculated with the Amsterdam density functional (ADF) program system,[43] developed by Baerends et al.[44,45] The electronic configurations of the molecular systems were described by a triple-ζ basis set on zirconium for 4s, 4p, 4d, 5s, and 5p. Double-ζ STO basis sets were used for carbon (2s, 2p) and hydrogen (1s), augmented with a single 3d and 2p function, respectively.[46,47] The inner shells on zirconium (including 3d) and carbon (1s) were treated within the frozen core approximation. Energetics and geometries were evaluated by using the local exchange-correlation potential by Vosko et al.,[48] augmented in a self-consistent manner with Becke's[49] exchange gradient correction and Perdew's[50,51] correlation gradient correction (BP86).

The ADF (Release 2.3) program was modified by one of us[52−54] to include standard molecular mechanics force fields in such a way that the QM and MM parts are coupled self-consistently.[55] The partitioning of the systems into QM and MM parts only involves the skeleton of the $Me_2C(3\text{-}t\text{-}Bu\text{-}1\text{-}Ind)_2$ ligand. The QM part of the $Me_2C(3\text{-}t\text{-}Bu\text{-}1\text{-}Ind)_2$ skeleton is represented by $H_2C(Cp)_2$. The only MM atoms, hence, are the methyl groups on the isopropyl bridge, and the carbon and hydrogen atoms needed to transform the pure QM $H_2C(Cp)_2$ skeleton into the QM/MM $Me_2C(3\text{-}t\text{-}Bu\text{-}1\text{-}Ind)_2$ ligand. The connection between the QM and MM parts occurs by means of the so-called capping "dummy" hydrogen atoms, which are replaced in the real system by the corresponding "linking" carbon atom. In the optimization of the MM part, the ratio between the sp^2-sp^2, sp^2-sp^3, and sp^3-sp^3 C−C bonds crossing the QM/MM border, and the corresponding optimized C−H distances, were fixed equal to 1.31, 1.39, and 1.40, respectively. The same partitioning scheme has been employed for test calculations involving the $C_2H_4(1\text{-Ind})$ ligand. Further details on the methodology can be found in previous papers.[52,54]

The MM potentials developed by Bosnich for bent metallocenes have been adopted.[56] This approach substantially corresponds to an extension of the Karplus CHARMM force field[57] to include group 4 metallocenes. For the atoms which are involved in reactive events at the active site, we followed the convention that atoms whose type changes during a reaction preserve the original type also in the transition state. For the transition states of the intermediate H-transfers to the metal involved in the epimerization reaction, however, we chose to describe the reacting carbon atoms with the "CT" type. All the structures which will follow are stationary points on the combined DFT/MM potential surface. Geometry optimizations were terminated if the largest component of the Cartesian gradient was smaller than 0.002 au. Transition-state geometries were approached by a linear-transit procedure, while all other degrees of freedom were optimized. Full transition-state searches were started from geometries corresponding to maxima along the linear-transit curves. As for geometry optimizations, transition state searches were terminated if the largest component of the Cartesian gradient was smaller than 0.002 au.

Results and Discussion

Chain Propagation Reactions and Stereoselectivity. Simple molecular mechanics calculations have provided a rationalization of the enantioselectivity of both heterogeneous and homogeneous catalysts and its dependence on the steric environment of the metal.[58−65] The origin of the enantioface selectivity is explained in terms of a "chiral orientation of the growing chain" (induced by the chiral ligand) which consequently discriminates between the *re* and the *si* monomer insertion. This model has correctly predicted that *ansa* C_2-symmetric zirconocenes in which the chirality of the π-ligand is *R,R* generally favor the insertion of *re* propene but also that single-carbon-bridged C_2-symmetric (*R,R*)-bis(3-R-Ind) zirconocenes will select the *si*-propene enantioface when R > CH_3, due to the stronger orientating effect the R group has on the growing chain with respect to the indenyl six-membered ring.[61] For this reason, we restricted the DFT/MM investigation of the propagation step and of the enantioselectivity on models comprising a *si*-ending chain. However, it has to be remarked that a number of studies[66,67] have shown that, in the presence of site control, the chirality of the last inserted unit plays a negligible role in the enantioselctive behavior of group 4 metallocenes. The only reason for including a chiral chain here is for the sake of comparison with the following sections.

Coordination of propene to the alkene-free species bearing a *si*-ending chain leads to the propene-bound states depicted in Figure 2. As for the *si*-propene

Downloaded by CARLI CONSORTIUM on June 29, 2009
Published on April 11, 2001 on http://pubs.acs.org | doi: 10.1021/om000680e

(42) Schlögl, K. *Top. Stereochem.* **1966**, 39.
(43) ADF 2.3.0; Vrije Universiteit Amsterdam, Amsterdam, The Netherlands, 1996.
(44) Baerends, E. J.; Ellis, D. E.; Ros, P. *J. Chem. Phys.* **1973**, *2*.
(45) te Velde, B.; Baerends, E. J. *J. Comput. Phys.* **1992**, *99*, 84.
(46) Snijders, J. G.; Baerends, E. J.; Vernooijs, P. *At. Nucl. Data Tables* **1982**, *26*, 483.
(47) Vernoijs, P.; Snijders, J. G.; Baerends, E. J. Department of Theoretical Chemistry, Free University Amsterdam, Amsterdam, 1981.
(48) Vosko, S. H.; Wilk, L.; Nusair, M. *Can. J. Phys.* **1980**, *58*, 0.
(49) Becke, A. *Phys. Rev. A* **1988**, *38*, 3098.
(50) Perdew, J. P.; Zunger, A. *Phys. Rev. B* **1986**, *33*, 8822.
(51) Perdew, J. P. *Phys. Rev. B* **1986**, *34*, 7406.
(52) Cavallo, L.; Woo, T. K.; Ziegler, T. *Can. J. Chem.* **1998**, *76*, 1457.
(53) Deng, L.; Woo, T. K.; Cavallo, L.; Margl, P. M.; Ziegler, T. *J. Am. Chem. Soc.* **1997**, *119*, 6177.
(54) Woo, T. K.; Cavallo, L.; Ziegler, T. *Theor. Chem. Acta* **1998**, *100*, 307.
(55) Maseras, F.; Morokuma, K. *J. Comput. Chem.* **1995**, *16*, 1170.
(56) Doman, T. N.; Hollis, T. K.; Bosnich, B. *J. Am. Chem. Soc.* **1995**, *117*, 1352.
(57) Brooks, B. R.; Bruccoleri, R. E.; Olafson, B. O.; States, D. J.; Swaminathan, S.; Karplus, M. *J. Comput. Chem.* **1983**, *4*, 187.
(58) Corradini, P.; Guerra, G.; Vacatello, M.; Villani, V. *Gazz. Chim. Ital.* **1988**, *118*, 173.
(59) Guerra, G.; Cavallo, L.; Moscardi, G.; Vacatello, M.; Corradini, P. *J. Am. Chem. Soc.* **1994**, *116*, 2988.
(60) Guerra, G.; Cavallo, L.; Moscardi, G.; Vacatello, M.; Corradini, P. *Macromolecules* **1996**, *29*, 4834.
(61) Toto, M.; Cavallo, L.; Corradini, P.; Moscardi, G.; Resconi, L.; Guerra, G. *Macromolecules* **1998**, *31*, 3431.
(62) Van der Leek, Y.; Angermund, K.; Reffke, M.; Kleinschmidt, R.; Goretzki, R.; Fink, G. *Chem. Eur. J.* **1997**, *3*, 585.
(63) Kawamura-Kuribayashi, H.; Koga, N.; Morokuma, K. *J. Am. Chem. Soc.* **1992**, *114*, 8687.
(64) Hart, J. A.; Rappé, A. K. *J. Am. Chem. Soc.* **1993**, *115*, 6159.
(65) Castonguay, L. A.; Rappé, A. K. *J. Am. Chem. Soc.* **1992**, *114*, 5832.
(66) Ewen, J. A. *J. Am. Chem. Soc.* **1984**, *106*, 6355.
(67) Balboni, D.; Moscardi, G.; Beruzzi, G.; Braga, V.; Camurati, I.; Piemontesi, F.; Resconi, L.; Nifant'ev, I. E.; Venditto, V.; Antinucci, S. *Macromol. Chem. Phys.*, in press.

Downloaded by CARLI CONSORTIUM on June 29, 2009
Published on April 11, 2001 on http://pubs.acs.org | doi: 10.1021/om000680e

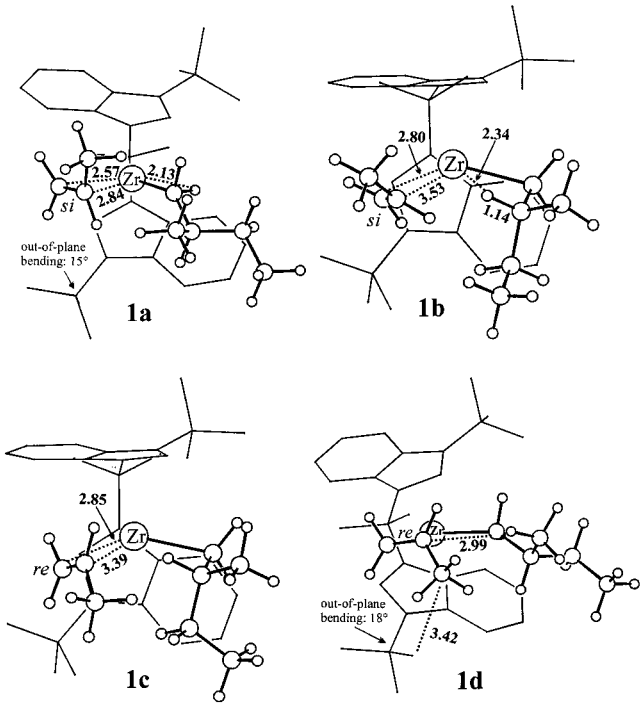

Figure 2. Optimized structures of $[L_2Zr(si\text{-chain})(propene)]^+$ (L_2 = (*R*,*R*)-Me_2C(3-*t*-Bu-1-Ind)$_2$) adducts showing β- and α-agostic chains and *re*- and *si*-coordinated propene. The hydrogen atoms on L_2 have been omitted for clarity.

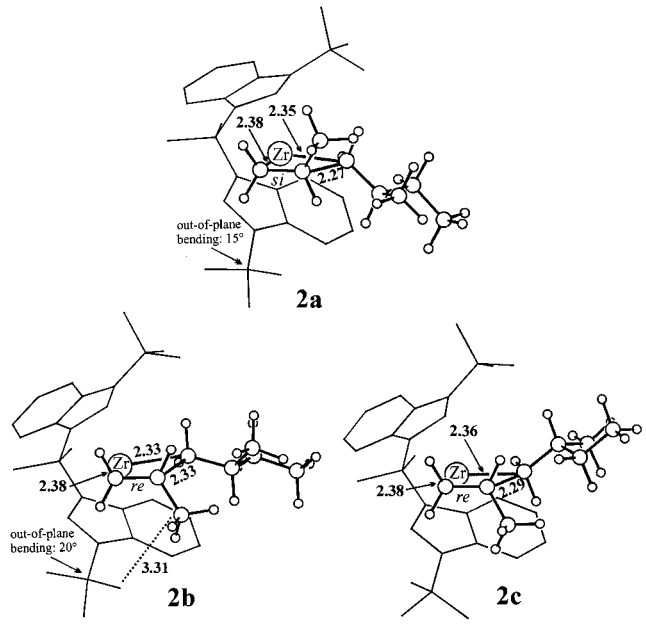

Figure 3. Transition states for propene insertion into a *si* chain: **2a** and **2c** show an *anti* relative placement of the growing chain and the CH_3 group of the *si*- and *re*-propene, respectively. Structure **2b** is relative to the *syn* placement of the mentioned groups.

coordination, structure **1a**, in which the chain is α-agostic, represents the most stable species, while its β-agostic conformer, **1b**, is 1.4 kcal/mol less stable. As for *re* propene coordination, the β-agostic intermediate **1c** lies 4.4 kcal/mol below the α-agostic species **1d** and is 1.8 kcal/mol above **1a**. The propene uptake energy from the most stable alkene-free species, which presents a γ-agostic bond (as we show further on), is 8.6 and 6.8 kcal/mol for **1a** and **1c**, respectively. This indicates that only under concentrated monomer conditions will the concentration of propene-bound intermediates be significantly increased relative to that of alkene-free species, since the moderate propene uptake energies do not counterbalance the unfavorable entropic factors.[68−70]

Several attempts to optimize propene-bound structures with a growing chain presenting a γ-agostic bond always converged into structures **1b** and **1c**, depending on the chirality of propene coordination. These findings are in agreement with results from other authors, which indicate that γ-agostic bonds are replaced by β-agostic ones prior to insertion.[71] Starting from the most stable propene-bound intermediates **1a** and **1c**, the insertion reaction can be thought to proceed through the three transition states **2a**, **2b**, and **2c**, depicted in Figure 3. According to our calculations, **2a** with a *si*-coordinated propene is the favored transition state, since **2b** and **2c**, both with a *re*-coordinated propene, lie 5.9 and 8.2 kcal/mol above **2a**, respectively. In agreement with our previous molecular mechanics analysis,[59−61] the transition state of lowest energy presents the growing chain oriented in a way that maximizes its distance from the bulkiest substituent on the metallocene skeleton (the *tert*-butyl group), and the inserting propene places its methyl group *anti* to (i.e., away from) the growing chain. For the unfavored *re* propene insertion, the path which proceeds through **2b**, with the propene methyl group *syn* (i.e., close) to the growing chain, is favored relative to **2c**, with a relative *anti* orientation of the mentioned groups. As for the activation barriers, the transition states **2a** and **2b** lie 0.6 and 4.7 kcal/mol above the favored propene-bound intermediates **1a** and **1c**, respectively.

The enantioselectivity, $\Delta\Delta E^{\ddagger}_{enant}$, calculated as the difference between the *re* and *si* insertion barriers, is 4.1 kcal/mol, while the energy difference between **2a** and **2b** is 5.9 kcal/mol. We recall that the experimental $\Delta\Delta E^{\ddagger}_{enant}$ value of 4.6 kcal/mol[2,3] is overestimated, since it does not take into account the contribution of chain-end epimerization (see above). Therefore, the calculated values of the enantioselectivity are in fair agreement with the experimental value. Since no regioirregular (2,1 or 3,1) internal propene units are experimentally observed, the regioselectivity of *propagation* of this catalyst has not been investigated. In any case, the high regioselectivity of the zirconocene based on the structurally related Me_2Si(3-*t*-Bu-1-Ind)$_2$ ligand has been rationalized in a previous paper.[61]

As a final remark, we note that the (*R*,*R*)-Me_2C(3-*t*-Bu-1-Ind)$_2ZrCl_2$-based catalysts is highly hindered, with a behavior somewhat different from that of the C_2-symmetric metallocenes studied so far. Two main aspects are worth noting. (1) In agreement with previous studies on similarly encumbered metallocenes, insertion of the *si* propene enantioface is favored for the *R*,*R* coordination of the Me_2C(3-*t*-Bu-1-Ind)$_2$ ligand. While the general prediction of enantioselectivity in favor of the *re* enantioface for metallocene complexes with π-ligand *R*,*R* coordinated has received several experi-

(68) Margl, P.; Deng, L.; Ziegler, T. *Organometallics* **1998**, *17*, 933.
(69) Musaev, D. G.; Froese, R. D. J.; Svensson, M.; Morokuma, K. *J. Am. Chem. Soc.* **1997**, *119*, 367.
(70) Moscardi, G.; Woo, T. K. Unpublished result of $-T\Delta S$ = 12 kcal/mol obtained for $(CH)_2(NH)_2NiC_3H_7(C_2H_4)^+ + C_2H_4$.
(71) Woo, T. K.; Margl, P. M.; Blöchl, P. E.; Ziegler, T. *J. Am. Chem. Soc.* **1996**, *118*, 13021.

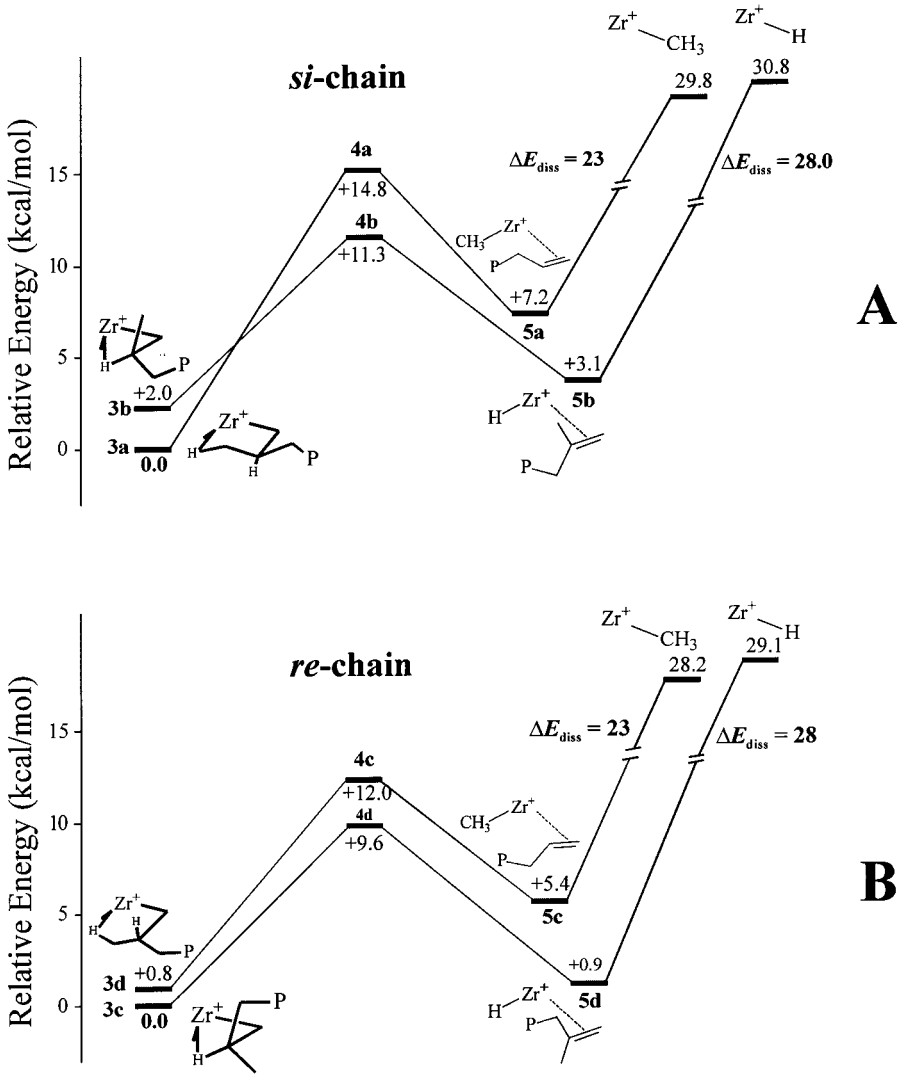

Figure 4. Comparison between the energy courses of the chain release mechanisms via unimolecular β-H and β-CH_3 (mechanisms a_1 and c_1) for the *si* chain (A) and *re* chain (B).

Downloaded by CARLI CONSORTIUM on June 29, 2009
Published on April 11, 2001 on http://pubs.acs.org | doi: 10.1021/om000680e

mental supports,[72−74] at the moment there is no experimental evidence of selectivity in favor of the *opposite* (*si*) propene enantioface for the *R,R* isomer of this catalyst. (2) According to our calculations, the monomer insertion leading to a stereomistake could proceed with a *syn* disposition of the β-C atom (and following carbons) of the polymer chain and the propene methyl group. This uncommon effect can be explained by the severe steric pressure exerted by the *tert*-butyl substituent on the growing chain. Approximate transition-state geometries with relative *syn* orientation of the aforementioned groups have been already considered in the past by some authors.[61,63,64]

Chain Release Reactions. In this section, we will investigate the chain release mechanisms leading to allyl and vinylidene chain end groups after insertion of the correct enantioface or after a stereomistake. This can be achieved by using *si*- and *re*-ending chains.

(a) Unimolecular Chain Release Reactions. The energy profiles for the β-hydride and the β-methyl transfer to the metal (mechanisms a_1 and c_1, respectively) starting from the alkene-free state including the *si* chain are summarized in Figure 4A and refer to the structures of Figure 5. The β-methyl transfer can be thought to proceed from the most stable alkene-free species **3a**, which is characterized by a γ-agostic interaction. The transition state **4a** lies 14.8 kcal/mol above **3a**. The product of the β-methyl transfer, **5a**, lies 7.2 kcal/mol above **3a** and presents a CH_3 group σ-bonded to the metal and a π-coordinated 1-butene molecule which simulates the terminated polymer chain. The β-hydride transfer to the metal, instead, proceeds from the alkene-free complex **3b** (presenting a β-agostic growing chain) through the transition state **4b**, 11.3 kcal/mol above the most stable alkene-free species **3a**, and terminates with the hydride adduct **5b** at 3.1 and 1.1 kcal/mol above **3a** and **3b**, respectively. This species can (1) start a sequence of double-bond reorientations/insertions, which will result in the epimerization of the chain end,[7] (2) dissociate the terminated chain, or (3) undergo allylic activation of the CH_3 or the CH_2P.[75]

The processes of β-methyl and β-H transfer may also

(72) Ewen, J. A.; Elder, M. J.; Jones, R. L.; Haspeslagh, L.; Atwood, J. L.; Bott, S. G.; Robinson, K. *Makromol. Chem., Macromol. Symp.* **1991**, *48*, 253.
(73) Pino, P.; Cioni, P.; Wei, J. *J. Am. Chem. Soc.* **1987**, *109*, 6189.
(74) Herzog, T. A.; Zubris, O. L.; Bercaw, J. E. *J. Am. Chem. Soc.* **1996**, *118*, 11988.
(75) Margl, P. M.; Woo, T. K.; Ziegler, T. *Organometallics* **1998**, *17*, 4997.

Downloaded by CARLI CONSORTIUM on June 29, 2009
Published on April 11, 2001 on http://pubs.acs.org | doi: 10.1021/om000680e

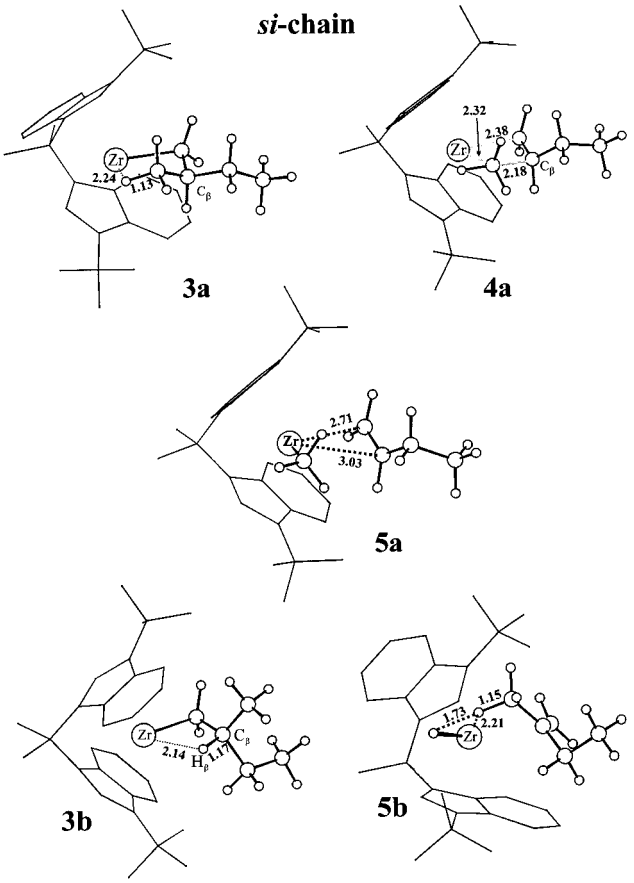

Figure 5. Optimized structures of the monomer free states showing γ- and β-agostic *si* chains (**3a** and **3b**, respectively), the transition state of the unimolecular β-CH_3 chain release process (**4a**), and the products of the unimolecular a_1 and c_1 chain release mechanisms (**5a** and **5b**).

occur after a stereomistake. Figure 4B shows the energy plot obtained for the unimolecular β-CH_3 and β-H transfers starting from alkene-free species including a *re* chain. The corresponding structures are reported in Figure 6. The β-methyl transfer proceeds from **3d** through the transition state **4c** at 12.0 kcal/mol above **3c** and terminates with the 1-butene adduct **5c**, at 5.4 kcal/mol above **3c**. The β-hydride elimination to the metal, instead, proceeds from **3c**, through the transition state **4d**, at 9.6 kcal/mol above **3c**, and terminates with the hydride adduct **5d**, at 0.9 and 0.1 kcal/mol above **3c** and **3d**, respectively.

When the plots of Figure 4 are compared, we see that the β-H transfer is the process with the lowest activation energy,[76] whatever the chirality of the chain, and that all the energy barriers are lower in the presence of a *re* chain. This suggests that the considered unimolecular chain transfer processes may have a higher probability to occur upon a stereomistake. It is worthy of note that the energies of these Zr−H(α,α-olefin) adducts are close to those of the related Zr−primary chain states **3a** and **3c**, respectively, due to the presence of agostic interactions. In particular, the agostic interaction in **5b** involves the CH_3 group, whereas that in **5d** involves CH_2−P. These results suggest that *si*- and *re*-ending chains will give rise to different Zr(allyl) species upon completion of hydrogen transfer and H_2 dissociation. We will discuss this topic later on.

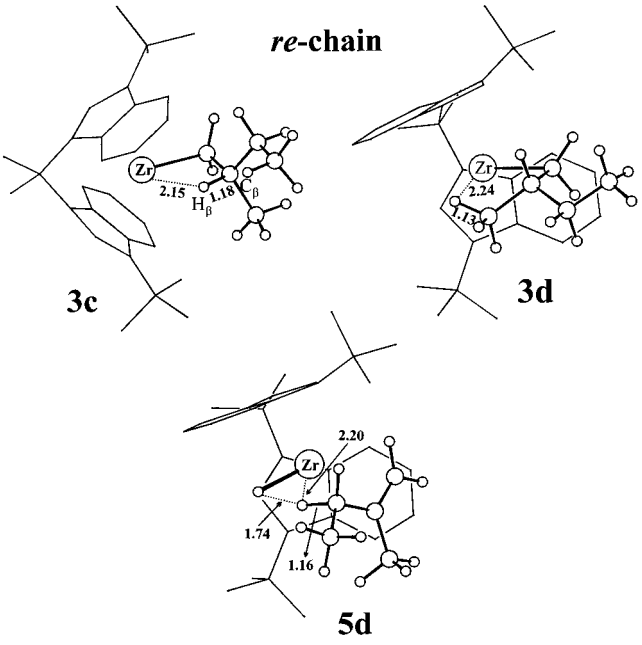

Figure 6. Optimized structures of the monomer free states showing β- and γ-agostic *re* chains (**3c** and **3d**, respectively) and the product of the unimolecular a_1 chain release mechanism (**5d**).

To conclude this section, we briefly discuss on the release of the terminated chain from the Zr−CH_3(1-butene) and the generic Zr−H(α,α olefin) states. We evaluate that dissociation of 1-butene from the products of the β-CH_3 transfer, **5a** and **5c**, leading to Zr−CH_3, requires almost 23 kcal/mol, while dissociation of 2-methyl-1-butene from the products of the β-H transfer, **5b** and **5d**, leading to Zr−H requires roughly 28 kcal/mol. Before comparing these numbers, it is important to note that these dissociation energies are largely overestimated, since solvent and/or counterion effects, as well as an unfavorable entropic $-T\Delta S$ contribution, have not been taken into account. Under conditions of low monomer concentration, the dissociation of the unsaturated polymer chain could be the most probable pathway. At present, we can only guess that within the approximation that both solvent and/or counterion stabilize $[Zr-H]^+$ and $[Zr-CH_3]^+$ to the same extent, the reaction path $Zr(C_5H_{11}) \rightarrow Zr-H$ + 2-methyl-1-butene will be slightly more endothermic than $Zr(C_5H_{11}) \rightarrow Zr-CH_3$ + 1-butene, whatever the nature of the polymer chain. This qualitatively gives an explanation for the experimental evidence[4] that $(k_{\beta-\text{methyl}} > k_{\beta-H})_{\text{uni}}$. Similar considerations were also developed by other authors.[77]

(b) Bimolecular Chain Release Reactions. The bimolecular β-hydride transfer reaction (mechanism a_2) can start from the β-agostic *re*- and *si*-monomer adducts **1b** and **1c** (sketched in Figure 2). The energy course of this reaction is plotted in Figure 7. The exchange of the β-H is assisted by the metal atom and proceeds through the transition states **6a** and **6b** (geometries shown in Figure 8) at 10.4 and 11.9 kcal/mol above **1b** and **1c**, respectively, to the chain transfer product **7** (also

(76) MacNeil, P. A.; Roberts, N. K.; Bosnich, B. *J. Am. Chem. Soc.* **1981**, *103*, 2273.

(77) Sini, G.; Macgregor, S. A.; Eisenstein, O.; Teuben, J. H. *Organometallics* **1994**, *13*, 1049.

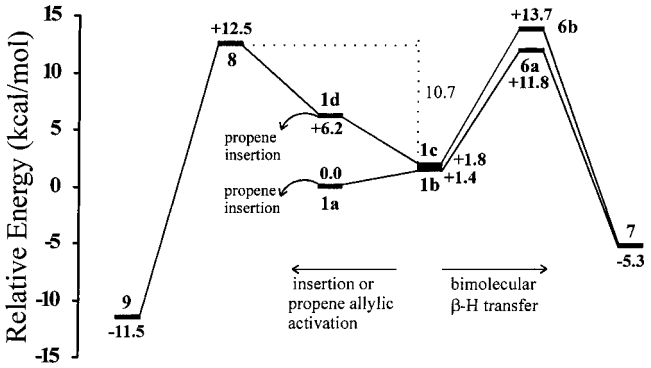

Figure 7. Comparison between the energy courses of the bimolecular chain release mechanisms via β-H exchange and allylic activation of a coordinated propene (mechanisms a_2 and c_3) for the *si* chain.

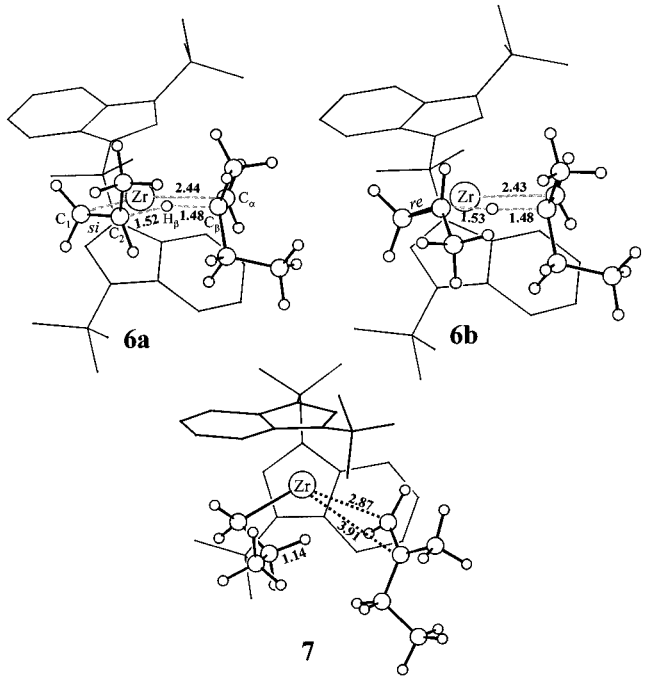

Figure 8. Transition states of the β-H transfer to the monomer (mechanism a_2) from the *si* chain involving *si*- and *re*-coordinated propene (**6a** and **6b**, respectively). Structure **7** depicts the chain release product.

sketched in Figure 8). Extremely similar results have been obtained from test calculations for the analogous reactions starting from the *re*-ending growing chain. The dissociation of 2-methyl-1-butene leading to the $Zr(C_3H_7)_{\beta-agostic}$ species requires 11.4 kcal/mol. The release of the terminated chain from **7** will most probably occur via dissociation, as a consequence of the favorable entropic factors. Moreover, a process of associative displacement by an incoming propene should occur via the *double* olefin adduct Zr(*n*-propyl)(propene)-(2-methyl-1-butene), which test calculations suggest to be sterically and energetically inaccessible.

We also attempted to model a bimolecular β-Me transfer (mechanism c_2) on the $[H_2C(Cp)_2Zr$-(*n*-propyl)-(ethene)$]^+$ model site. In particular, the transition state of Figure 9 had high energy, more than 60 kcal/mol with respect to a β-agostic ethene-bound state. This result dissuaded us from investigating this issue further.

Finally, we also investigated the chain release reaction through allylic activation of a coordinated propene

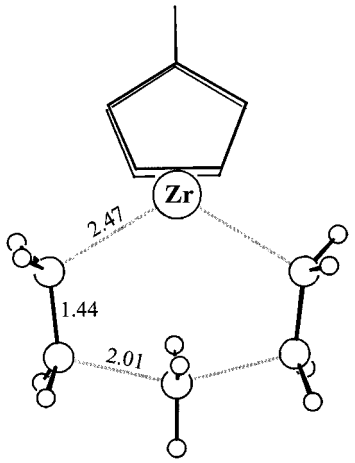

Figure 9. Transition state of the bimolecular β-CH_3 transfer (mechanism c_2) from the $[H_2C(Cp)_2Zr$(ethyl)-(ethene)$]^+$ model site. Hydrogen atoms on the ligand framework have been omitted for clarity.

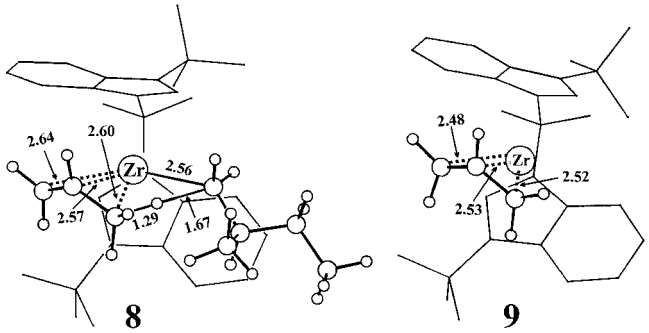

Figure 10. Transition state and product (**8** and **9**, respectively) of the allylic activation of a *re*-coordinated propene (mechanism c_3).

molecule[28−31] (c_3), supported by the evidence, both experimental and theoretical,[2,75,78−80] that zirconocene catalysts may propagate the chain growth on Zr−allyl η^3 bonds. Theoretical studies on the activation of the C−H bonds have also been reported in the literature.[81,82] With the *si*-propene adduct **1d** as the starting compound, the allylic activation of propene proceeds through the transition state **8** and terminates with the Zr(η^3-allyl) species **9**, sketched in Figure 10. The transition state is stabilized by the early allylic-type interaction between the metal center and the reacting propene. Indeed, test calculations performed by choosing orientations of the monomer that exclude this interaction resulted in transition states of much higher energy. The transition state **8** is related to the *re*-propene adduct **1c**, and its energy is 10.7 kcal/mol above that of the latter. An analogous transition state obtained starting from the *si*-monomer adduct **1b** resulted of somewhat higher energy (by nearly 2.5 kcal/mol). These results indicate that *the propene coordination which would generate a stereomistake will more easily undergo allylic*

(78) Richardson, D. E.; Alameddin, N. G.; Ryan, M. F.; Hayes, T.; Eyler, J. R.; Siedle, A. R. *J. Am. Chem. Soc.* **1996**, *118*, 11244.
(79) Karol, F. J.; Kao, S.; Wasserman, E. P.; Brady, R. C. *New J. Chem.* **1997**, *21*, 797.
(80) Lieber, S.; Prosenc, M.; H.; Brintzinger, H. H. **1999**, *19*, 377.
(81) Rabaâ, H.; Saillard, J.-Y.; Hoffmann, R. *J. Am. Chem. Soc.* **1986**, *108*, 4327.
(82) Ziegler, T.; Folga, E.; Berces, A. *J. Am. Chem. Soc.* **1993**, *115*, 636.

Downloaded by CARLI CONSORTIUM on June 29, 2009
Published on April 11, 2001 on http://pubs.acs.org | doi: 10.1021/om000680e

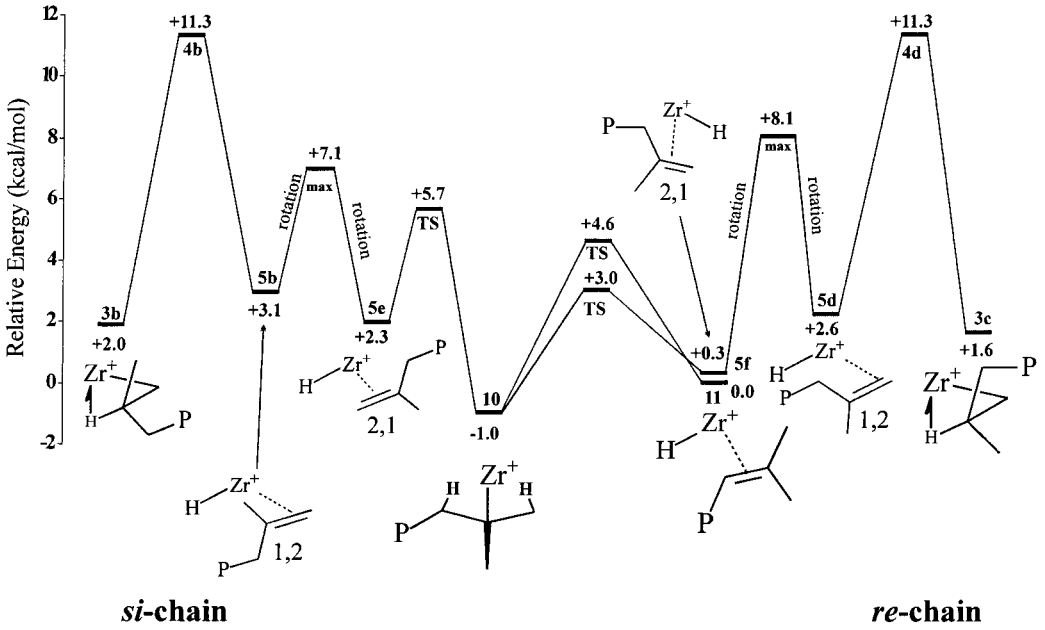

Figure 11. Energy profile of the epimerization reaction and formation of the isobutenyl chain-end group via H-transfer form the CH_2 of the intermediate tertiary alkyl species (mechanism b_1). Energies are relative to that of the γ-agostic conformer of the *si* chain (structure **3a**).

activation. This mechanism could be in any case competitive with that of bimolecular β-H transfer, thus suggesting that the allyl group may also be a chain-initial one, rather than chain-end only. Moreover, this mechanism also requires propene insertion into a Zr−allyl η^3-bond to restart the catalytic cycle. This step is feasible at high monomer concentration, as Ziegler has shown for the polymerization of ethene.[75] We will discuss the enantioselectivity of the insertion step later on.

We conclude the section of the primary chain release reactions by observing that all the bimolecular mechanisms investigated in this work (plot of Figure 7) proceed with activation energies at least of 11 kcal/mol higher with respect to that of the "right" propene insertion. Assuming that under monomer-rich conditions the bimolecular chain release reactions are largely prevailing, our estimated value of $\Delta\Delta E^{\ddagger}_{\text{release-insertion}}$ is in line with the measured one of 10.7 kcal/mol[2,3] in liquid monomer.

Epimerization Reaction. This reaction inverts the configuration of the methine of the last inserted unit; that is, it converts a *si*-ending chain into a *re*-ending one in a unimolecular process. In the framework of this paper, it corresponds to convert structure **3b** into **3c**. Other authors[83−85] have already theoretically investigated the epimerization mechanism as proposed by Busico.[7] The plot of Figure 11 shows the sequence of β-H transfers/olefin reorientations/reinsertions which connects **3b** and **3c**. In Figure 12 some of the intermediates are shown. It is worth noting that the *secondary* (2,1) Zr−H(α,α-olefin) adducts **5e** and **5f** and the tertiary alkyl species **10** are stabilized by agostic interactions, where the latter is *double* agostic. The

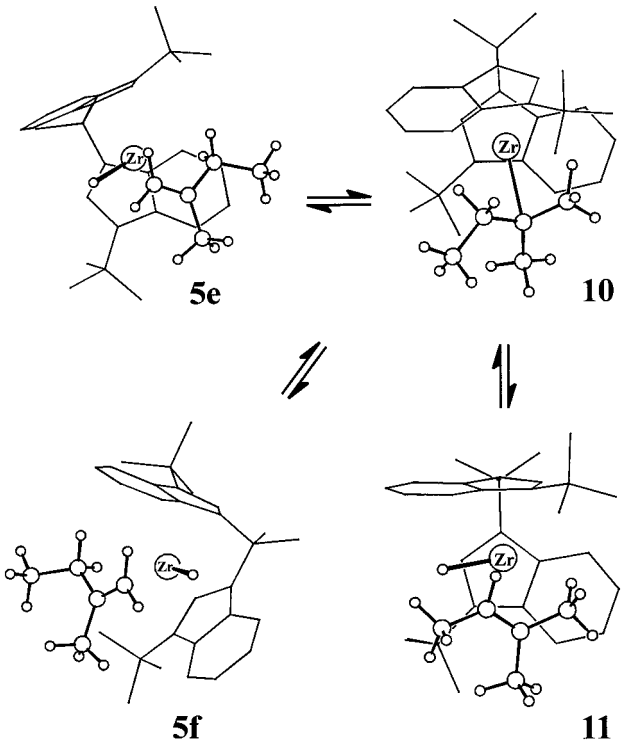

Figure 12. Structures of relevant intermediates in the chain-end epimerization reaction. The Zr−H(2,1-olefin) intermediate (**5e**) gives rise to a tertiary alkyl species which can undergo β-H transfer toward the isobutenyl chain-end group (**5f**) or a new Zr−H(2,1-olefin) intermediate (**11**) which will complete the epimerization.

steps **3b** → **5b** and **5d** → **3c** are rate-determining, while the other steps of H reinsertion and abstractions (**5e** → **10** and **10** → **5f**) have much lower activation energies, since we found that the agostic interactions in **5e** and **10** are preserved at the transition states. Other authors[83] proposed a mechanism of olefin flip which exchanges the coordination chirality of the *primary* (1,2) α,α-olefin (that is, from **5b** to **5d** in our case) without

(83) Prosenc, M. H.; Brintzinger, H. H. *Organometallics* **1997**, *16*, 3889.
(84) Thorshaug, K.; Støvneng, J. A.; Rytter, E.; Ystenes, M. *Macromolecules* **1998**, *31*, 7149.
(85) Lohrenz, J. C. W.; Buhl, M.; Thiel, W. *J. Organomet. Chem.* **1999**, *592*, 11.

Downloaded by CARLI CONSORTIUM on June 29, 2009
Published on April 11, 2001 on http://pubs.acs.org | doi: 10.1021/om000680e

requiring the formation of a tertiary alkyl intermediate. We have calculated a barrier of nearly 11 kcal/mol for this process. Therefore, at least with **1**, a stepwise mechanism with the tertiary alkyl species **10** as intermediate seems to be favored.

The above energy profiles could provide a rationalization of the higher degree of epimerization observed for **1**/MAO, with respect to **2**/MAO (see experimental data above). Toward this aim, we have investigated the process of β-H transfer from the $[C_2H_4(1\text{-Ind})_2Zr\text{-}re\text{-chain}]^+$ species[86] and evaluated that the transition state and the product are 9.0 and 7.2 kcal/mol above the β-agostic state, respectively. The product, in particular, is not stabilized by any agostic interaction, as happens in **5b**. This effect can be related to the wider framework provided by the $Me_2C(3\text{-}t\text{-Bu-1-Ind})_2$ ligand,[87] which can more easily accommodate the bulky 2-methyl-1-butene olefin. Therefore, β-H transfer to Zr could have a higher degree of reversibility in the presence of the $C_2H_4(1\text{-Ind})_2$ ligand. Since we consider these findings adequate to rationalize the different behavior of the two catalysts, we did not investigate the remaining part of the epimerization reaction in the presence of the $C_2H_4(1\text{-Ind})_2$ ligand.

Before concluding, it is worthy to note that the tertiary alkyl species **10** can be considered as a precursor for the formation of the isobutenyl end groups (mechanism b_1) In fact, if β-H elimination from **10** occurs from the CH_2 group, this intermediate evolves toward the Zr−H(2-Me-2-butene) species **11**, in which the 2-methyl-2-butene molecule simulates the isobutenyl-terminated polymer chain. This chain release reaction **10** → **11** requires a barrier of 5.6 kcal/mol, which is only 1.6 kcal/mol higher than the barrier for the step **10** → **5f** needed to proceed on the epimerization path.

Allylic Activations. As anticipated in the unimolecular chain release section, following the β-hydride transfer to the metal, the resulting $Zr-H(CH_2{=}C(CH_3)(CH_2CH_3)$ species can undergo allylic activation (mechanism d_1), either from the CH_3 or the CH_2, generating the $Zr(H_2)(\eta^3\text{-2-P-allyl})$ (P = polymer) and $Zr(H_2)(\eta^3\text{-1-P-2-methylallyl})$ species, respectively. As shown by Ziegler and co-workers,[75] the allylic activation is generally quite facile. The plots in parts A and B of Figure 13 show the energy courses of the allylic activations associated with the *si* and the *re* chains, respectively.

As for allylic activations from the *si* chain, the pathway of lowest activation energy is that which will lead to the formation of the $Zr(H_2)(\eta^3\text{-2-P-allyl})$ species **12a**. Allylic activations of each H atom of CH_2 were found to have higher activation energies and less stable products, namely **12b** and **12c**. In particular, the energy barrier needed to form **12c** is similar to that required to reverse the β-H transfer reaction back to the starting species **3a**. In the case of allylic activations from the *re* chain instead, the most favored process is that leading to the formation of the $Zr(H_2)(\eta^3\text{-}syn\text{-1-P-2-methylallyl})$ species **12d**. Molecular hydrogen is thought to dissociate quite easily from the generic $Zr(H_2)(\eta^3\text{-allyl})$ species[75] (generating the species **13a** and **13b** shown in Figure 14, respectively) since the entropic effects substantially counterbalance the coordination enthalpy of H_2, which we evaluate to be equal to 9.2, 8.1, and 6.9 kcal/mol for **12a**, **12b**, and **12d**, respectively. In agreement with previous studies,[75] the highest energy barrier for the formation of the generic $Zr(\eta^3\text{-allyl})$ species is that required by the transfer of the first β-hydrogen from the saturated chain to the zirconium center. In a recent paper,[80] Brintzinger and co-workers have studied both the rotation and the haptotropic rearrangement of the

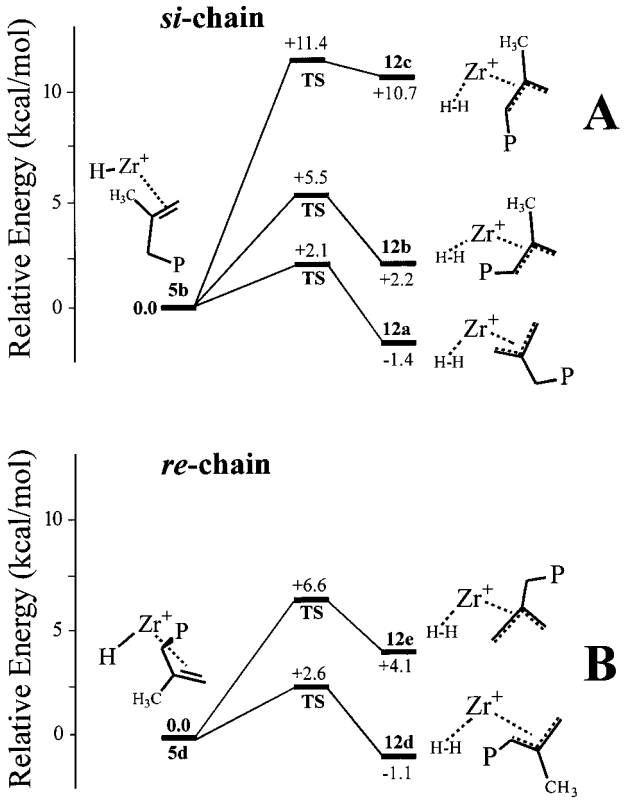

Figure 13. Comparison between the energy courses of the chain release mechanisms via unimolecular allylic activation (mechanism d_1) for the *si* chain (A) and *re* chain (B).

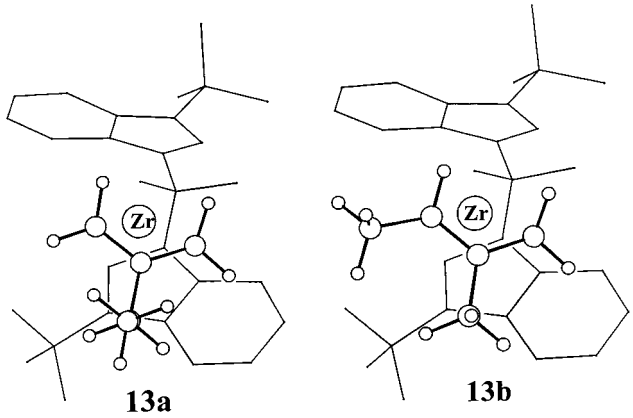

Figure 14. Optimized structures of the $[L_2Zr(\eta^3\text{-2-P-allyl})]^+$ and $[L_2Zr(\eta^3\text{-}syn\text{-1-P-2Me-allyl})]^+$ species (L_2 = (R,R)-$Me_2C(3\text{-}t\text{-Bu-1-Ind})_2$).

(86) According to previous calculations,[59] the *primary* (1,2) propene insertion on the $(R,R)C_2H_4$(1-Ind)-based zirconocene occurs prevalently with its *re* enantioface. Therefore, we restricted this study to the *re* chain only.

(87) The angle between the mean planes of the five-membered rings in the $[L_2Zr-H(2\text{-Me-2-butene})]^+$ complex is nearly 74° for $L_2 = (R,R)$-$Me_2C(3\text{-}t\text{-Bu-Ind})_2$ and 59° for $L_2 = (R,R)$-C_2H_4(1-Ind). The angles centroid(C_5)−Zr−centroid(C_5') are nearly 117 and 126° for the two ligands, respectively.

(88) Wasserman, E. P.; Hsi, E.; Young, W.-T. *Polym. Prepr. Am. Chem. Soc., Div. Polym. Chem.* **1998**, *39*, 425.

Downloaded by CARLI CONSORTIUM on June 29, 2009
Published on April 11, 2001 on http://pubs.acs.org | doi: 10.1021/om000680e

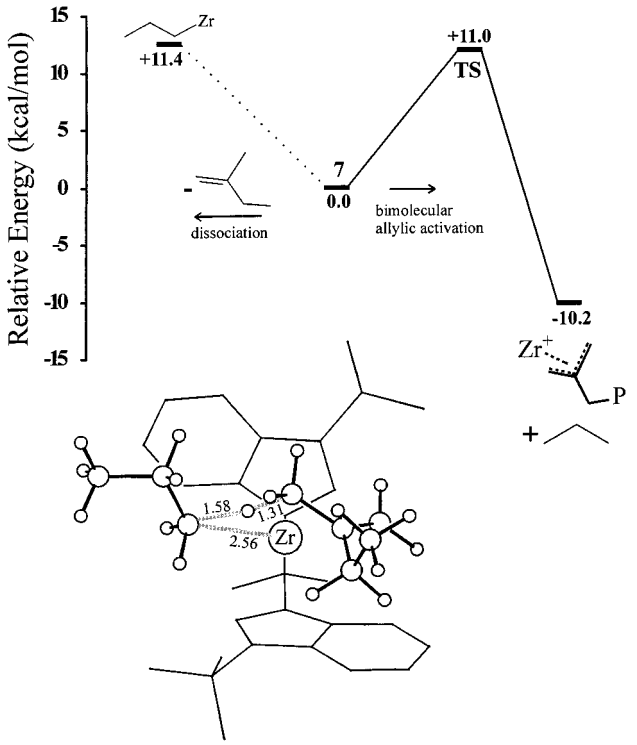

Figure 15. Comparison between the energy courses of the competing bimolecular allylic activation of the polymer chain (solid line, mechanism d_2) and dissociation (dotted line) of the terminated chain upon β-H transfer to the monomer. The structure depicts the transition state of mechanism d_2.

allyl ligand in the $[(Cp)_2Zr(\eta^3\text{-methallyl})]^+H_3CB(C_6F_5)_3^-$ complex. From these results, we can also postulate a relatively facile conversion of the H_2-free allylic species formed from **12b** into the more stable (by 2.6 kcal/mol) H_2-free allylic species **13a**.

To summarize, our analysis suggests that the *si* chain will most probably give rise to the $Zr(\eta^3\text{-2-P-allyl})$ species, while the $Zr(\eta^3\text{-}syn\text{-1-P-2-Me-allyl})$ species is expected from the *re* chain. Finally, it is worth noting that due to the previously discussed uncertainity of the stability of the Zr−H(olefin) species, it is not easy to compare the probabilities for the product of the unimolecular β-hydride elimination to undergo dissociation or allylic activation.

The above results are based on the assumption that the allylic activation is a unimolecular process. Indeed, molecular hydrogen has been detected during ethene or propene polymerization.[27,79,88] However, a *bimolecular* course (mechanism d_2, as an extension of Marks' mechanism) can be postulated by considering that the product of the β-H transfer to the monomer (structure **7** in Figure 8) can be a precursor of a further transfer of the H atom of the CH_3 or the CH_2 of the olefin to the *n*-propyl group, thus forming the $Zr(\eta^3\text{-2-P-allyl})$ or the $Zr(\eta^3\text{-1-P-2-methylallyl})$ species, respectively, and releasing a propane molecule. In other words, *the allylic activation of the chain could also occur without developing molecular hydrogen*. The plot of Figure 15 shows that the activation energy of the transfer from the CH_3 is almost equal to the dissociation energy of the terminated chain. The structure of the transition state is also depicted in the same figure. We believe that this further activation could compete with the dissociation, since the entropic factors can be assumed to be nearly the same, but the activation reaction is much more exothermic. Unimolecular and bimolecular allylic activations may be competing processes; that is, the unimolecular process could predominate at low monomer concentration. At present, however, the occurrence of the bimolecular course has to be assumed only as a working hypothesis, supported only by calculations. Its experimental confirmation would be difficult at best, since propane is always present (up to 5%) in the propene used for polymerization tests.

Reactivation of Allylic Species. Internal unsaturations are generated by chain propagation from the generic allylic species upon H_2 dissociation. The insertion step of propene onto the $[(Cp)_2Zr(\eta^3\text{-methallyl})]^+$ species has been recently described by Prosenc and Brintzinger, [80] who also indicated that the preferred insertion pathway is that proceeding from the methallyl η^3-coordinated to the metal. In the following, we describe the insertion step of both *re* and *si* propene enantiofaces onto the allyl, the 2-P-allyl and the *syn*-1-P-2-methylallyl species being η^3-bonded to the metal center (structures **11**, **13a**, and **13b**, respectively). In particular, the chain propagation restart from Zr^+(allyl) is required to complete the chain release reaction upon allylic activation of propene (see previous section) and that from Zr^+-(2-P-allyl) to account for the internal vinylidene unsaturations.

For all the species considered, our attempts to optimize structures including a coordinated propene molecule to the generic $Zr^+(\eta^3\text{-allyl})$ complexes always resulted in electrostatic adducts, stabilized by 5.7, 5.1, and 4.3 kcal/mol with respect to **11**, **13a**, and **13b** plus free propene, respectively, with a substantially uncoordinated monomer ($Zr-C_2 \geq 5$ Å). As a comparison, Ziegler and co-workers[75] reported an uptake energy of 10 kcal/mol for the coordination of ethene to $[Ph_2C(Cp\text{-}9\text{-}Flu)Zr(\eta^3\text{-1-methylallyl})]^+$, and Brintzinger found nearly 7 kcal/mol for the uptake energy of propene to the $[(Cp)_2Zr(\eta^3\text{-methallyl})]^+$ fragment.[80] As shown by other authors,[75] inclusion of zero point energy corrections and entropic factors indicate that only in liquid monomer are the concentrations of the adducts significantly increased relative to that of the monomer-free species **11**, **13a**, and **13b**. To model the propene insertion from the adducts originating from **11** and **13a**, we shrunk the CH(propene)−CH_2(allylic growing chain) distance and found the transition states **14a** and **14b** and **14c** and **14d**, in Figure 16, which lie at 7.9 and 10.6 and at 7.6 and 9.7 kcal/mol above the related propene adducts, respectively. The calculated insertion barriers are between those (5.5 and 14.5 kcal/mol) reported by Ziegler[75] and Brintzinger.[80] The difference between the energies of **14a** and **14b**, 2.6 kcal/mol, and those of **14c** and **14d**, 2.1 kcal/mol, suggests a relatively scarce enantioface selectivity in favor of the *si* monomer enantioface, in good agreement with the experimental data.[4] As it happens for the propagation step over the saturated chain, the *si* monomer enantioface is the "right" one also in the case of the generic $Zr(\eta^3\text{-allyl})$ species.

The propagation step proceeding from **13b** has been investigated in the case of the *si* propene only. Quite higher activation energies, 15.5 and 13.6 kcal/mol, were calculated for propene attack at the CH(P) or at the CH_2

Downloaded by CARLI CONSORTIUM on June 29, 2009
Published on April 11, 2001 on http://pubs.acs.org | doi: 10.1021/om000680e

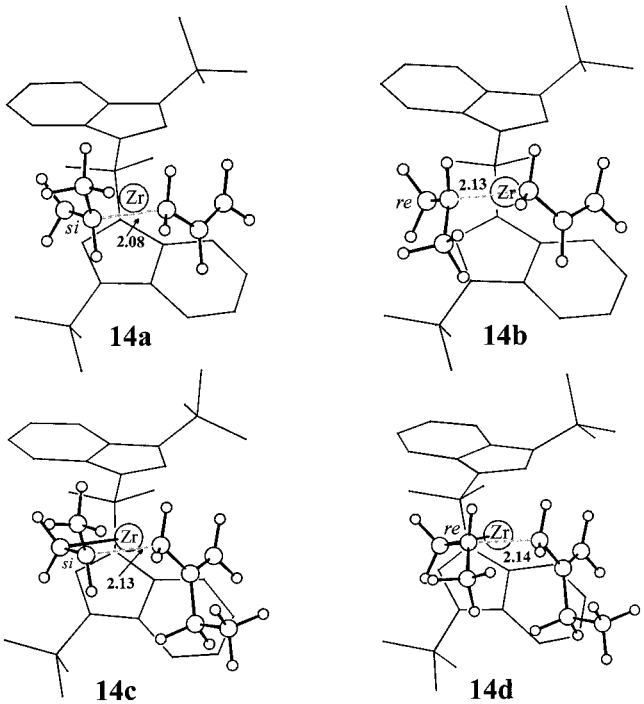

Figure 16. Transition states of the insertion step into $[L_2Zr(\eta^3\text{-allyl})]^+$ and $[L_2Zr(\eta^3\text{-2-P-allyl})]^+$ in which *si*- and *re*-coordinated propenes are involved (L_2 = (*R*,*R*)-Me_2C(3-*t*-Bu-1-Ind)$_2$).

groups of *syn*-1-P-2-methylallyl, respectively. This can be explained with the steric hindrance of the *syn*-1-P-2-methylallyl group. These findings are in line with the experimental data[4] that clearly rule out the presence of internal unsaturations of the type $-CH_2C(Me)=CH-CH(Me)-$. Moreover, the substantial independence of the molecular weight on the Al/Zr ratio rules out the hypothesis of a chain transfer to aluminum to explain the formation of the isobutenyl group. In our opinion, the allylic species **13b** could be inert enough to accumulate over time and eventually, in the absence of alkyl/allyl exchange with the Al cocatalyst,[80] would lead to deactivation of the catalyst.

Conclusions

The available experimental data on the polymerization performances of **1**/MAO have been reviewed. A theoretical analysis carried out on the chain propagation step and on possible mechanisms for the formation of unsaturations in propene polymerization allowed us to conclude the following

(1) The two possible propene insertions (namely, the "right" one, and the "wrong" one that leads to the stereoerror) proceed through transition states having the polymer chain oriented in the same direction (specifically, as far as possible from the bulky substituent). This occurs because in the "wrong" propene insertion, the steric repulsions between the chain and the ligand framework that would arise in an *anti* insertion transition state are higher than those between the propene methyl group and the chain placed *syn* in a transition state of lower energy (compare structures **2b** and **2c** in Figure 3). This finding may reflect a possible general behavior of the very sterically crowded catalysts. Moreover, it is also worth noting that in both the propene-bound and the insertion transition state for the "wrong" insertion, short nonbonding distances between the *t*-Bu group and the methyl of propene are present despite a large bending of the *t*-Bu out of the Ind plane (see the structures in Figures 2 and 3). This suggests that catalyst enantioselectivity can also be influenced by a *direct* steric pressure on the monomer, rather than on the growing chain only.

(2) The relatively high rate of chain-end epimerization, which in the case of **1**/MAO occurs already in liquid monomer, and the presence of internal vinylidene groups can be rationalized with the relatively high stability of the product of the β-H transfer to the metal. Previous theoretical studies on this chain release mechanism[75,83−85] always evidenced a more flat potential energy surface once the transition state is overcome, the Zr−H(olefin) state being 2−4 kcal/mol lower in energy than the transition state. Therefore, it was obvious to postulate a short lifetime of the Zr−H(olefin) state. In this case, in contrast, the energy barrier required to reverse the β-H transfer back to the Zr primary chain state is higher (plot of Figure 11) than that required to proceed along the remainder of the epimerization path (or, alternatively, to undergo allylic activation/H_2 release and monomer insertion to give the internal vinylidene). Calculations indicate that this could not be the case for **2**/MAO. Finally, it is worth noting that the $Zr-C(CH_3)_2P$ tertiary alkyl intermediate is even more stable than the primary $Zr-CH_2CH(CH_3)P$ species, thus providing a further driving force toward the epimerization and confirming the mechanism originally proposed by Busico.[7] These results are in agreement with those obtained by Lohrenz on a nonenantioselective system.[85] Due to the very labile $Zr-H_2$ interaction, allylic activation followed by H_2 reinsertion, proposed by one of us earlier, is less likely to be the source of epimerization.[27]

(3) As outlined in the Introduction, the nonlinear activity/[M] relationship can be explained by a single-center, two-state catalyst model,[5] where the active metal centers can exist in two states, having different propagation rate constants, which can interconvert without monomer assistance. The nature of the fast and the slow states has not yet been clarified. In part 1 of this work,[32] we have shown that the Zr(isopropyl) site has a high chain propagation barrier, compared to that calculated for the Zr(*n*-propyl) site. Analogously, the tertiary alkyl species arising during the course of the epimerization is expected to behave in the same way. These observations allow us, contrary to what has been suggested earlier by one of us,[27] to propose that the fast site is the primary $Zr-CH_2CH(CH_3)P$, whatever the nature of its agostic interaction with the metal center, while the tertiary alkyl state seems to satisfy all the above requirements for being the resting state of the catalyst.

(4) Allylic activation of the chain end, followed by propene insertion (mechanism d_1), causes formation of internal vinylidene unsaturations.

(5) The large amount of allyl chain end groups at any [M] can be rationalized with the occurrence, especially at the highest monomer concentrations, of a reaction of allylic activation of the coordinated propene. Allyl end groups formed by this route add to those formed by the

Downloaded by CARLI CONSORTIUM on June 29, 2009
Published on April 11, 2001 on http://pubs.acs.org | doi: 10.1021/om000680e

known unimolecular β-Me transfer. This process kinetically competes with the chain release by β-H transfer to the monomer and, interestingly, also with the insertion step which will give rise to a stereomistake. We are aware of the fact that this allylic activation of the coordinated propene, originally proposed by Marks,[28,30,31] contradicts the experimental results observed in the oligomerization of propene *in liquid propene* with $Cp^*_2ZrCl_2$/MAO, where allylic end groups have been unambiguously assigned to unimolecular β-Me transfer.[20]

Allylic chain end activation could also occur upon β-H transfer to a coordinated monomer. This means that the vinylidene-terminated polymer chain could have a certain probability to further react, as an alternative to the dissociation, with formation of internal vinylidenes without developing H_2.

Acknowledgment. We thank Dr. Giuseppe Milano of Università di Salerno (Salerno, Italy) for the study on the bimolecular β-CH_3 transfer and other test calculations and Dr. Fabrizio Piemontesi of Basell for useful discussions and helpful suggestions. L.C. thanks the MURST of Italy for PRIN grants in 1999 and 2000.

OM000680E

Downloaded by CARLI CONSORTIUM on June 29, 2009
Published on April 11, 2001 on http://pubs.acs.org | doi: 10.1021/om000680e